Femtosecond filamentation of optical vortices for the generation of optical air waveguides

Silin Fu, Benoît Mahieu, André Mysyrowicz, Aurélien Houard

Femtosecond filamentation of optical vortices for the generation of optical Air waveguides

Silin Fu, Benoit Mahieu, Andre Mysyrowicz, and Aurelien Houard*

[1] *Laboratoire d'Optique Appliquée - ENSTA Paris, Ecole Polytechnique, CNRS, Institut Polytechnique de Paris, Palaiseau, France*
**Corresponding author: aurelien.houard@polytechnique.edu*

We study the filamentation in air of multi-millijoule optical vortices and compare them with the classical filamentation regime. The femtosecond vortex beam generates multiple plasma filaments organized in a cylindrical geometry. This plasma configuration evolves into a meter scale tubular neutral gas column that can be used as a waveguide for nanosecond laser pulses at 532 nm. It appears that optical vortices produce a more uniform heating along the propagation axis, when compared to gaussian or supergaussian beams, and that the resulting low-density channel is poorly sensitive to the laser input power thanks to the combination of filamentation intensity clamping and phase vorticity.

Femtosecond laser filamentation allows projecting high light intensities over extended lengths in the atmosphere, up to kilometric distances [1-4]. Through the optical Kerr effect, self-focusing of the laser beam occurs during propagation and eventually light intensities in the range 10^{13}-10^{14} W/cm^2 are reached, high enough to ionize air molecules. A long and continuous plasma string is thus left in the wake of the laser pulse. Filamentation appears spontaneously provided the pulse peak power exceeds a critical value $P_{cr} \approx$ 7-10 GW in air at 800 nm [2], but filament intensity and the amount of laser energy deposited in the medium strongly depends on the initial peak power and numerical aperture of the beam [5-6]. Typically, increasing the initial beam focusing strength for a fixed peak power will reduce the filamentation length and increase its intensity.

Many applications have been proposed for these light filaments such as the laser lightning rod [7-10], multispectral LiDAR [11] remote backward lasing for sensing [12], cloud clearing for telecommunications [13] and waveguiding for THz or optical pulses [14-17]. For many applications it is desirable to organize the spatial distribution of multiple filaments that are produced when the initial laser power $P > P_{cr}$. It can be done using amplitude or phase masks [18-19]. Demonstration of filamentation has been reported with Bessel beams [20], spatially curved airy beams [21-22], or more recently with Laguerre Gaussian beams, also called vortex beams [23-27]. These vortex beams are particularly interesting because they can generate a stable ring profile with a rotating phase. This phase momentum makes them more suitable for telecommunications through atmospheric turbulences [28]. It also allows the organization of multiple filaments in a cylindrical shape that is optimal to guide electromagnetic waves.

Polynkin *et al.* have demonstrated that femtosecond vortex beams can collapse to form a ring of individual filaments, provided the input pulse power is higher than $1.7mP_{cr}$, where P_{cr} is the critical power for self-focusing and m the topological order of the vortex [24-25]. The term of helical filament has also been used to describe these filaments since this array of filament has been shown to rotate during propagation, due to the phase vorticity of the beam [26-27]. Vortex filaments could find application in the guiding of microwaves or THz waves [14] or act as a guide for optical waves [16].

In this work we study the filamentation of femtosecond vortex beams with an energy of 25 mJ weakly focused in air (Numerical aperture (NA) = 0.0025) and compare them with classical filaments produced by a supergaussian beam of same energy. We analyze the shape of the generated plasma and of the ensuing low-density air channel and measure the deposition of energy by the vortex beam in air for different laser pulse durations. Finally, we demonstrate that vortex filaments can be used as a guide for a nanosecond laser pulse at 532 nm.

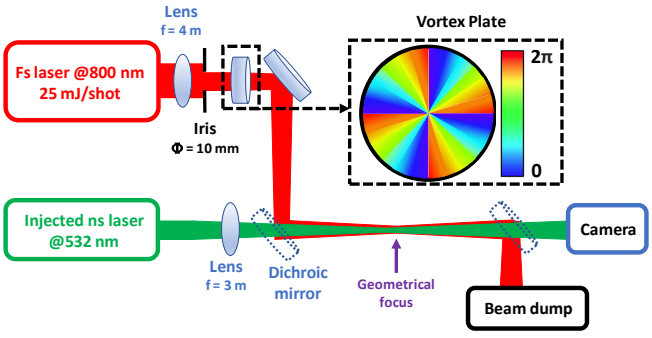

Fig. 1. Experimental setup used for the optical waveguide experiment.

The laser used to produce the optical vortex is a chirped-pulse amplified Ti:Sapphire laser system from Amplitude Technologies. It can deliver laser pulses at 800 nm with 200 mJ energy, 50 fs duration at a repetition rate of 10 Hz. For this study the laser beam was limited by an iris to a diameter of 10 mm resulting in a super-gaussian profile with energy of 25 mJ. The pulse duration was adjusted from 50 fs to 2 ps by detuning the grating compressor of

the laser to add positive chirp. The beam was then focused by a convex lens with focal length f = 4 m and a diffractive vortex plate with topological order m = 4 from Holo/Or was inserted on the beam path to produce the helical phase pattern.

To test the ability of tubular filaments to act as an optical guide, we built the setup shown in Fig. 1. A probe beam at 532 nm with µJ-level energy and 10 ns pulse duration was delivered by a Yb:YAG laser, synchronized with the Ti:Sapphire fs laser system. The delay between the two lasers could be controlled using a digital delay generator. A dichroic mirror was used to combine the two beams and glass color filters to block the 800 nm beam after the filament. The profile of the probe beam at 532 nm was imaged by a CMOS camera placed 4 meters after the geometrical focus of the beams.

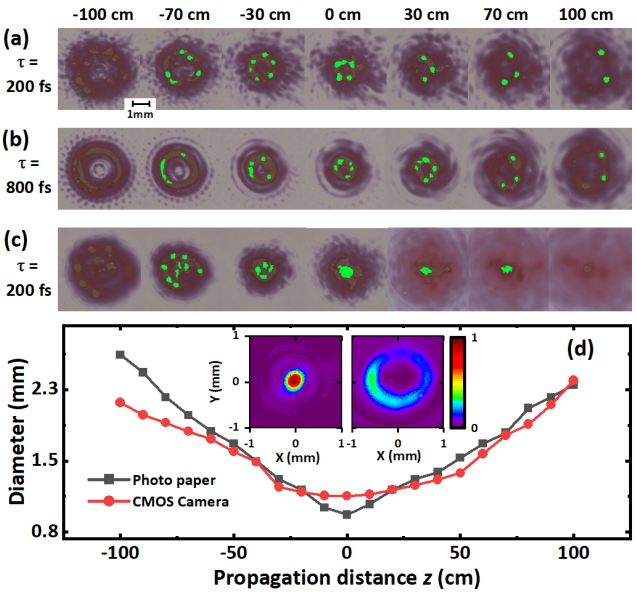

Fig. 2. Beam profile measured as a function of the propagation distance z by impact on photosensitive paper for a vortex beam with 25 mJ energy and a duration of 200 fs (a) and 800 fs (b) and for a supergaussian beam with duration 200 fs (c). z = 0 is to the linear focus of the lens. (d) Diameter of the ionized ring measured at high intensity with τ = 200 fs (black curve) and diameter of the intensity ring measured at low intensity by a CMOS camera (red curve) as a function of z. The inset compares the low intensity profile measured at the focus for a supergaussian and a vortex beam.

We first characterized the propagation of the focused optical vortices at low energy (E ≈ µJ) using a CMOS camera and at high energy (E = 25 mJ) using photosensitive paper. Fig. 2(a) presents the evolution of the beam profile along the propagation axis z measured with photosensitive paper. The green color indicates the burned area of the paper, corresponding to filament formation. For a pulse with duration τ = 200 fs (P = 160 GW ≈16 P_{cr}), we observe between 3 and 6 distinct filaments organized in a circle over a distance of 1.5 m around the geometrical focus. The diameter of this ionized circle matches well the diameter of the low intensity vortex beam up to z = -25 cm and then becomes slightly smaller over 70 cm after the focus (see Fig. 2(d)). This contraction might be explained by Kerr self-focusing appearing at high intensity. When the initial laser pulse duration τ is chirped from 200 to 800 fs (P = 36 GW) the number and the length of the filaments produced are decreased.

As shown by [29-30] the formation of long-lived low-density channels resulting from filamentation is directly related to the density of energy deposited inside the filament through ionization and Raman absorption. To characterize the deposition of energy by the vortex filament we used a broadband microphone GRAS Model 46BH ¼" placed on the side of the beam at a distance of 20 mm. This microphone measures the transverse pressure wave generated by the filament that is proportional to the density of deposited energy in filaments. The result is presented in Fig. 3(a) for a vortex beam and for a supergaussian beam with the same input energy. For a vortex beam with 200 fs duration a quasi-constant signal is measured over 1 meter from z = -90 to +25 cm. The supergaussian beam shows a signal 5 times higher with a peak over 30 cm, typical from a regime of superfilamentation [5].

The total energy deposition in the vortex filaments was measured as a function of the laser input pulse duration τ (Fig. 3(b)). We can see that this energy deposition is decreased by a factor 2 when the laser pulse duration is increased from 200 fs to 800 fs and remains then quasi constant around 1.3 mJ for longer pulse durations. We note that the total energy deposited with the supergaussian beam is only 30 % higher than the vortex one, while the ratio of their acoustic signals is about 3 to 4. Considering that the shape of the energy deposition follows the measured pressure wave presented in Fig. 3(a) we can estimate the maximum lineic energy deposition to be 95 µJ/cm for the supergaussian beam and 52 µJ/cm for the vortex beam. Therefore, despite the much lower intensity generated at the focus by the vortex beam, the energy deposition of the vortex beam is comparable to the one produced by the supergaussian beam, taking into account its larger mode.

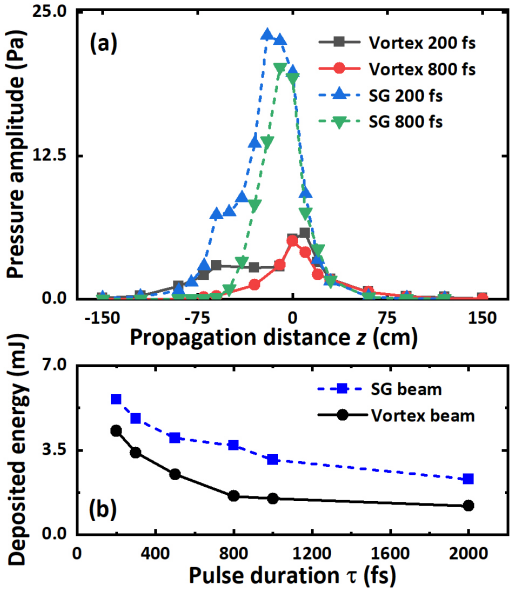

Fig. 3. (a) Amplitude of the lateral acoustic wave measured by the microphone 20 mm away from the beam for the 25 mJ, laser pulse. (b) Energy deposited in the filament for an input pulse energy of 25 mJ for a supergaussian beam (blue curve) and a vortex (m = 4) beam (black curve) as a function of the laser pulse duration.

The temporal evolution of the vortex filaments after plasma recombination was characterized using transverse interferometry by means of a probe laser with 10 µs duration at a wavelength of

640 nm, whose phase profile was analyzed by a Phasics SID4HR wavefront sensor (see ref. [31] for a description of the setup). The plane x = 0 containing the propagation axis is imaged on the sensor to get the profile of the gas density in this plane. Fig. 4 presents the phase shift measured on the vortex filament after 1 µs (a) and 500 µs (b). At 1 µs one can see 4-5 distinct low-density channels generated by filaments with a ~100 µm size. After 500 µs these filaments broaden to form two low-density channels with a 300 µm width. We note that magnitude of the phase variations measured with 200 fs and 800 fs pulse were very similar. This can be explained by the mechanism of intensity clamping inside the filament. The phase shift profile integrated along z is also plotted in Figs. 4(c) and 4(d) for delays of 1 µs and 500 µs, respectively. The phase shift produced by the vortex beam is compared to the one produced by the supergaussian beam. One can see that the phase difference is only 50% higher for the supergaussian case with a gaussian density profile, while the vortex generates a hollow profile. Assuming an axial symmetry around Z axis at long delays, we calculated the corresponding air density modulation after 500 µs (Fig. 4(e)) using Abel inversion [30]. One can see that the air density profile generated by the vortex beam is similar to a step-index fiber with a maximum density on the laser axis, explaining why it is beneficial for guiding.

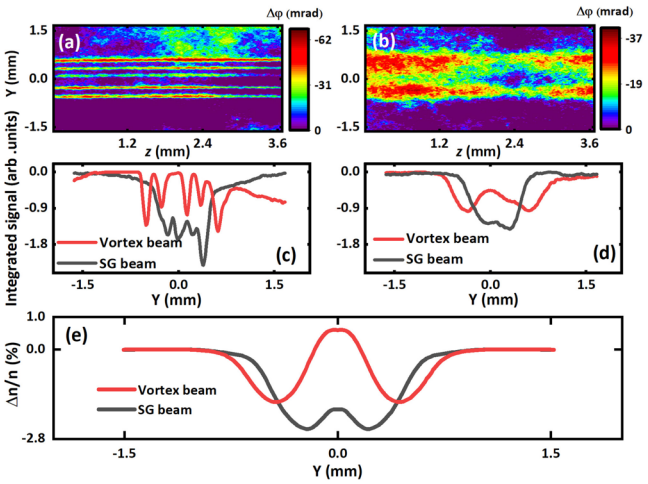

Fig. 4. Transverse image of the filaments produced by the vortex beam with 800 fs duration measured 1 µs (a) and 500 µs (b) after the filament formation at position z = -30 cm obtained by interferometry. (c) Phase shift Δφ integrated along z for a delay of 1 µs (c) and 500 µs (d) for a supergaussian beam (black curve) and a vortex beam (red curve). Air density variations corresponding to the phase in Fig. 4(e).

We then tested the ability of the vortex filaments to act as a long-lived air waveguide by injecting a nanosecond laser probe with an energy ~10 µJ at 532 nm in the tubular low-density channel. Similar waveguides were first demonstrated by Jhaj *et al.* using an array of four filaments [16]. The beam profile of the probe laser in the absence of the femtosecond laser is presented in Fig. 5(a), with a gaussian profile and a width of 9 mm FWHM. The output profile of the 532 nm beam in the presence of the vortex beam is then presented for different delays Δt between the fs vortex beam and the ns probe beam, ranging from 2 µs to 2 ms. For delays of a few µs, the probe beam is perturbed by the vortex beam but no guiding is observed. But for Δt ranging from 100 µs to 1 ms an intense spot with a width of 1.5 mm can be observed in the beam profile, signature of a laser guiding effect. We define the guided energy as the percentage of laser energy in a circle of 5 mm diameter, corresponding to the guided mode (see red circle in the fig. 5(c)). The percentage of guided energy in this mode is plotted in Fig. 5(f) as a function of the probe delay Δt and in Fig. 5(g) as a function of the pulse duration of the vortex beam. The guiding is maximum for a delay of 500 µs and lasts for a millisecond, similar to the results of ref. [16] with an array of 4 filaments. Surprisingly, the guiding efficiency does not depend on the vortex pulse duration (or peak power). This result is in agreement with the interferometric measurements made for different laser pulse durations. Indeed, as shown in Fig. 3(a) increasing the peak power of the vortex beam extends the filaments toward the laser, but will not modify the guiding part around and after the focus. In addition, an advantage compared to the waveguide produced by 4 filaments is the scalability of the vortex since the diameter of the guide can be increased with the topological order of the waveplate (or by decreasing the beam numerical aperture), while adjusting the input laser energy.

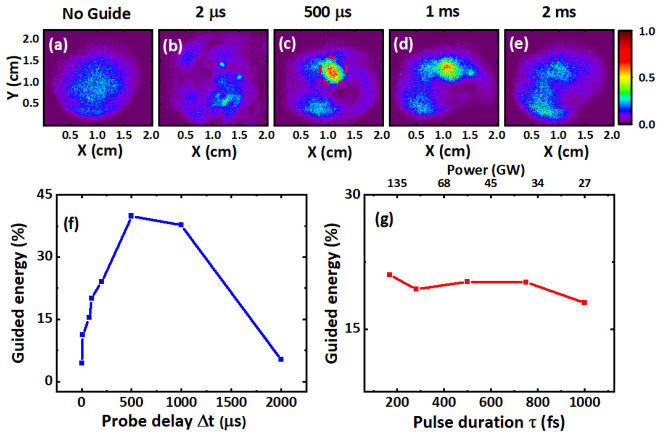

Fig. 5. Far field profile of the probe beam measured 4 m after the geometrical focus in the absence of vortex beam (a) and in the presence of vortex beam for delays of 1 µs (b), 500 µs (c), 1 ms (d) and 2 ms (e). (f) Percentage of guided energy as a function of the delay Δt between the two pulses (f) and as a function of the pulse duration τ of the input vortex pulse for a delay of 100 µs (g).

In this article, we analyzed the propagation and temporal hydrodynamic evolution of energetic vortex beams in air in weakly focused conditions. We showed that multiple filaments appear in an annular beam, whose diameter is mainly governed by the topological order and the numerical aperture of the beam. Compared to the filaments of classical Gaussian beams, vortex beams produce a more uniform ionization and deposition of energy along z. Also, despite the fact that ionization rate and density of deposited energy are significantly smaller with the vortex, the lineic deposited energy and the induced low-density channels are comparable between vortex and supergaussian optical pulses.

The hollow core structure imposed by the vortex phase makes the vortex filaments array ideal to act as a guiding structure for terahertz waves [32] or optical pulses. This waveguide can be easily

scalable by increasing the input laser energy and appears to be weakly sensitive to the laser input peak power.

Funding. S. F. acknowledges funding from the Chinese Scholarship Council.

Acknowledgments. Authors acknowledge M. Lozano, X. Zhang and P. Walch for their technical support.

Disclosures. The authors declare no conflicts of interest.

Data availability. Data underlying the results presented in this paper are not publicly available at this time but may be obtained from the authors upon reasonable request.

References

1. S. L. Chin, S. A. Hosseini, W. Liu, Q. Luo, F. Théberge, N. Aközbek, A. Becker, V. P. Kandidov, O. G. Kosareva, and H. Schröder, Canadian Journal of Physics **83**, 863 (2005).
2. A. Couairon, A. Mysyrowicz, "Femtosecond filamentation in transparent media," Phys. Rep. **441**, 47-189 (2007).
3. M. Rodriguez, R. Bourayou, G. Méjean, J. Kasparian, J. Yu, E. Salmon, A. Scholz, B. Stecklum, J. Eislöffel, U. Laux, A. P. Hatzes, R. Sauerbrey, L. Wöste, and J.-P. Wolf, "Kilometer-range nonlinear propagation of femtosecond laser pulses," Phys. Rev. E **69**, 036607 (2004).
4. M. Durand, A. Houard, B. Prade, A. Mysyrowicz, A. Durécu, B. Moreau, D. Fleury, O. Vasseur, H. Borchert, K. Diener, R. Schmitt, F. Théberge, M. Chateauneuf, J.-F. Daigle and J. Dubois, "Kilometer range filamentation," Opt. Express **21**, 26836 (2013).
5. G. Point, Y. Brelet, A. Houard, V. Jukna, C. Milián, J. Carbonnel, Y. Liu, A. Couairon, and A. Mysyrowicz, "Superfilamentation in Air," Phys. Rev. Lett. **112**, 223902 (2014).
6. K. Lim, M. Durand, M. Baudelet, and M. Richardson, "Transition from linear- to nonlinear-focusing regime in filamentation," Sci. Rep. **4**, 7217 (2014).
7. H. Pépin, D. Comtois, F. Vidal, C. Y. Chien, A. Desparois, T. W. Johnston, J. C. Kieffer, B. La Fontaine, F. Martin, and F. A. M. Rizk, "Triggering and guiding high-voltage large-scale leader discharges with sub-joule ultrashort laser pulses," Physics of Plasmas **8**, 2532 (2001).
8. P. Rambo, J. Schwarz and J.-C. Diels, "High-voltage electrical discharges induced by an ultrashort-pulse UV laser system," J. Opt. A **3**, 146 (2001).
9. T. Produit, P. Walch, C. Herkommer, A. Mostajabi, M. Moret, U. Andral, A. Sunjerga, M. Azadifar, Y.-B. André, B. Mahieu, W. Haas, B. Esmiller, G. Fournier, P. Krötz, T. Metzger, K. Michel, A. Mysyrowicz, M. Rubinstein, F. Rachidi, J. Kasparian, J.-P. Wolf, A. Houard, "The Laser Lightning Rod project," The European Physical Journal Applied Physics **93**, 10504 (2021).
10. A. Houard, P. Walch, T. Produit, V. Moreno, B. Mahieu, A. Sunjerga, C. Herkommer, A. Mostajabi, U. Andral, Y.-B. André, M.Lozano, L. Bizet, M. C. Schroeder, G. Schimmel, M. Moret, M. Stanley, W. A. Rison, O. Maurice, B. Esmiller, K.Michel, W.Haas, T. Metzger, M. Rubinstein, F. Rachidi, V. Cooray, A. Mysyrowicz, J. Kasparian, J.-P. Wolf, "Laser-guided lightning," arXiv:2207.03769 (2022).
11. J. Kasparian, M. Rodriguez, G. Méjean, J. Yu, E. Salmon, H. Wille, R. Bourayou, S. Frey, Y.-B. André, A. Mysyrowicz, R. Sauerbrey, J.-P. Wolf, "and L. Wöste, Science **301**, 61 (2003).
12. P. N. Malevich, R. Maurer, D. Kartashov, S. Ališauskas, A. A. Lanin, A. M. Zheltikov, M. Marangoni, G. Cerullo, A. Baltuška, and A. Pugžlys, "Stimulated Raman gas sensing by backward UV lasing from a femtosecond filament," Opt. Lett. **40**, 2469-2472 (2015).
13. G. Schimmel, T. Produit, D. Mongin, J. Kasparian, and J.-P. Wolf, "Free space laser telecommunication through fog," Optica **5**, 1338-1341 (2018).
14. M. Châteauneuf, S. Payeur, J. Dubois, and J.-C. Kieffer, "Microwave guiding in air by a cylindrical filament array waveguide", Appl. Phys. Lett. **92**, 091104 (2008).
15. Z. Kudyshev, M. Richardson, & N. Litchinitser, "Virtual hyperbolic metamaterials for manipulating radar signals in air," Nat. Commun. **4**, 2557 (2013).
16. N. Jhajj, E. W. Rosenthal, R. Birnbaum, J. K. Wahlstrand, and H. M. Milchberg, "Demonstration of long-lived high-power optical waveguides in air," Phys. Rev. X **4**, 011027 (2014).
17. E. W. Rosenthal, N. Jhajj, J. K. Wahlstrand, and H. M. Milchberg, "Collection of remote optical signals by air waveguides," Optica **1**, 5-9 (2014).
18. G. Méchain, A. Couairon, M. Franco, B. Prade, and A. Mysyrowicz, "Organizing Multiple Femtosecond Filaments in Air," Phys. Rev. Lett. **93**, 035003 (2004).
19. D. V. Pushkarev, A. S. Lar'kin, E. V. Mitina, N. A. Zhidovtsev, D. S. Uryupina, R. V. Volkov, S. V. Karpeev, S. N. Khonina, A. A. Karabutov, Yu. E. Geints, O. G. Kosareva, and A. B. Savel'ev, "Robust multifilament arrays in air by Dammann grating," Opt. Express **29**, 34189-34204 (2021).
20. P. Polesana, M. Franco, A. Couairon, D. Faccio, and P. Di Trapani, "Filamentation in Kerr media from pulsed Bessel beams," Phys. Rev. A **77**, 043814 (2018).
21. P. Polynkin, M. Kolesik, J.V. Moloney, G.A. Siviloglou, D.N. Christodoulides, "Curved plasma channel generation using ultraintense Airy beams." Science **324**, 229 (2009).
22. P. Panagiotopoulos, D. Papazoglou, A. Couairon, and S. Tzortzakis, "Sharply autofocused ring-Airy beams transforming into non-linear intense light bullets," Nat. Commun. **4**, 2622 (2013).
23. G. A. Swartzlander and C. T. Law, "Optical vortex solitons observed in Kerr nonlinear media," Phys. Rev. Lett. **69,** 2503 (1992).
24. P. Polynkin, C. Ament, and J.V. Moloney, "Self-Focusing of Ultraintense Femtosecond Optical Vortices in Air," Phys. Rev. Lett. **111**, 023901 (2013).
25. M. Burger, P. Polynkin, and I. Jovanovic, "Filament-induced breakdown spectroscopy with structured beams," Opt. Express **28**, 36812-36821 (2020).
26. N. Barbieri, Z. Hosseinimakarem, K. Lim, M. Durand, M. Baudelet, E. Johnson, M. Richardson, "Helical filaments," Appl. Phys. Lett. **104**, 261109 (2014).
27. L. Xu, D. Li, J. Chang, Z. Hao, "Helical filaments array generated by femtosecond vortex beams with lens array in air," Results in Physics **25**, 104334 (2021).
28. W. Chen, J. Haus, Q. Zhan, "Propagation of vector vortex beams through a turbulent atmosphere," Opt. Express **17**, 17829 (2009).
29. J. K. Wahlstrand, N. Jhajj, E. W. Rosenthal, S. Zahedpour, and H.M. Milchberg, "Direct Imaging of the Acoustic Waves Generated by Femtosecond Filaments in Air," Opt. Lett. **39**, 1290 (2014).
30. G. Point, C. Milián, A. Couairon, A. Mysyrowicz, and A. Houard, Generation of long-lived underdense channels using femtosecond filamentation in air, J. Phys. B **48**, 094009 (2015).
31. P. Walch, B. Mahieu, L. Arantchouk, Y.-B. Andre, A. Mysyrowicz, and A. Houard, "Cumulative air density depletion during high repetition rate filamentation of femtosecond laser pulses: Application to electric discharge triggering," Appl. Phys. Lett. **119**, 264101 (2021).
32. M. Alshershby, J. Lin, Z. Hao, "Numerical analysis of guiding a microwave radiation using a set of plasma filaments: dielectic waveguide concept," J. Phys. D: Appl. Phys. **45**, 065102 (2012).